Parameter Analysis of Crisscross Shaped Concrete Filled Steel Tube Columns under Axial Loading

Aleesha Theresa Vithayathil, Gokul Raveendran K, Nithin Mohan

Abstract— Criss-cross shaped concrete-filled steel tube (XCFST) columns are becoming attractive to researchers and engineers owing to their advantages of avoiding column protrusion from walls and they can save space. In addition, these columns can be used as central columns in civil engineering applications. Numerous research studies have been conducted on the behaviour of these types of columns under axial compression; however, the design methods require further investigations. In this study, finite element (FE) models of cross-shaped composite column connected by double vertical steel plates were developed to simulate the axial behaviour and parameter analysis. By conducting 3D nonlinear analysis using ANSYS Workbench, the effect of width of connecting plates over the load carrying capacity of crisscross shaped columns are studied. Maximum allowable ratio between width of mono column and that of connecting plate and maximum allowable ratio between the length of the column and overall breadth are determined.

Index Terms— concrete-filled steel tube columns, criss-cross shaped columns, FE analysis, parameter analysis.

1 INTRODUCTION

COMPOSITE construction may be considered as a reliable choice of attaining proper balance between the advantages it offers and the cost. An extensive variety of composite columns are available nowadays, but the concrete filled steel tubular (CFST) sections are the most commonly used one. CFST member is an innovative idea; a hollow tubular member is filled with concrete, used as columns that are appropriate replacement for hot-rolled steel (or) reinforced concrete (RC) members in structural systems of tall buildings and bridges. This composite system utilizes the compressive strength of the concrete and the steel tube lies in the outer limits contributes a large portion of the stiffness and tensile strength, in addition, it provides required confinement to the concrete core, which increases the compressive strength of the column member.

In compression, CFST short column reaches their ultimate capacity when both the steel and the concrete reach their strength limit point, i.e., yielding of the steel and crushing of the concrete and the CFST slender columns are governed by stability and failed by column buckling. The CFST structural member has a number of distinct advantages over a steel and reinforced concrete member. Owing to their structural benefits such as reduced cross section, high strength, improved fire resistance, greater apparent stiffness and excellent seismic resistant structural properties like high ductility and energy absorption, the use of CFST columns has become increasingly popular in construction of building structures. Furthermore, the steel tube of CFST member can serve as formwork during infilling of concrete. The inward local buckling commonly observed in bare steel tubes, is effectively prevented and eliminated in CFST member (Fig.1). There is also no need for the use of shuttering during concrete construction; hence, the construction cost and time are reduced.

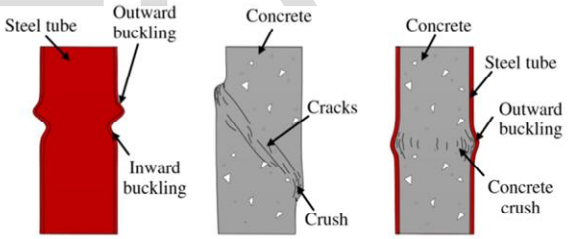

Fig.1 Schematic failure modes of hollow steel tube, concrete and CFST stub columns

2 SPECIAL SHAPED CFST COLUMNS

CFST columns with circular, square and rectangular sections have been commonly used in numerous engineering structures due to their excellent composite actions between steel tube and concrete infill. The main drawback for conventional shaped columns is column protrusion and thus they reduce the usable building area. Fig. 2 shows the application rectangular cross-sectional column in a frame structure.

To satisfy aesthetic requirements, various types of novel columns have been widely used and studied all around the world. In recent years, special shaped CFST (SCFST) columns, mainly L-shaped (LCFST), T-shaped (TCFST) and cross-shaped (XCFST) have been increasingly used in engineering

- *Aleesha Theresa Vithayathil is currently pursuing masters degree program in structural engineering in APJ Abdul Kalam Technological University, India, PH-9961381355. E-mail: aleesha.theresa@gmail.com*
- *Gokul Raveenran K is currently workingas assistant professor in civil engineering department, Vidya Academy of Science and Technology, Kerala, India, PH-9995888501. E-mail: gokul.r.k@vidyaacademy.ac.in*
- *Nithin Mohan is currently workingas assistant professor in civil engineering department, Vidya Academy of Science and Technology, Kerala, India, PH-8086673523. E-mail: nithin.m@vidyaacademy.ac.in*

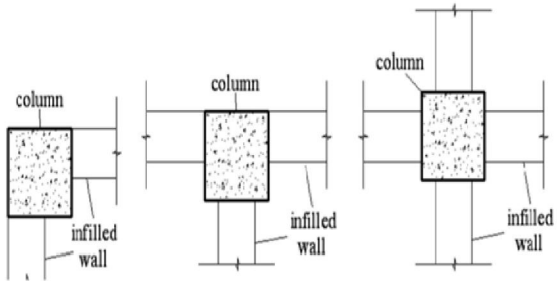

Fig. 2. Rectangular cross-sectional columns in frame structure

structures as single columns or as edge members of shear walls, on account of their convenient constructions at beam–column joints, larger moments of inertia of cross-sections and better satisfaction with architectural requirement compared with regular-shaped (such as circular, square or rectangular) CFST sections, as well as superior strength, ductility and seismic behaviour over special-shaped RC columns.

An L-shaped CFST column is composed of three small-sized concrete filled square tubular columns called mono-columns; a T-shaped CFST column is composed of four of these mono-columns; and a cross-shaped CFST column is composed of five mono columns. The mono-columns are connected by connection plates and are embedded in walls, as shown in Fig. 3 and Fig. 4.

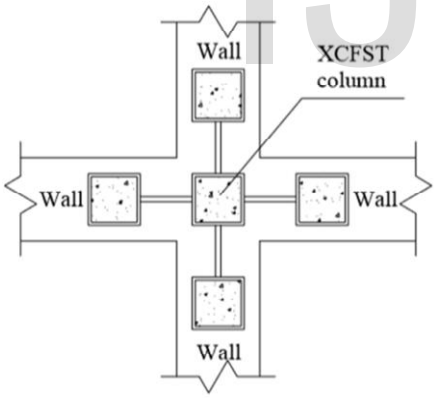

Fig. 3. : Cross-shaped CFST column

3 CONNECTING PATTERNS IN SCFST COLUMNS

In SCFST columns, mono-columns are connected each-other in-order to act as a single column using different types of connecting patterns. Broadly saying, there are three types of connecting systems in SCFST columns. Double vertical steel plate connection (Fig. 5), single vertical steel plate connection (with or without circular holes) (Fig. 6 and Fig. 7) and lacing bar connection (Fig. 8).

In recent years, several studies were conducted comparing these connecting systems. It has been shown that double vertical steel plate connection has better contribution than the other two, in increasing the ultimate load carrying capacity of the SCFST columns.

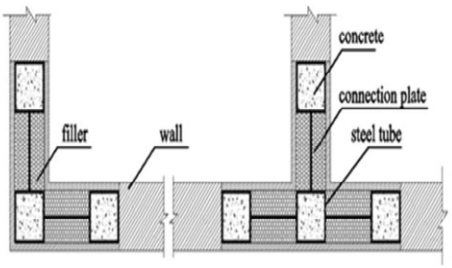

Fig. 4. L-shaped and T-shaped CFST columns

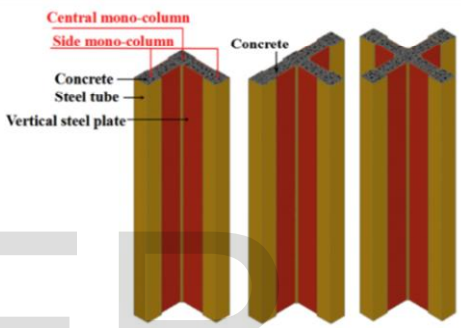

Fig. 5. Double vertical steel plate connection

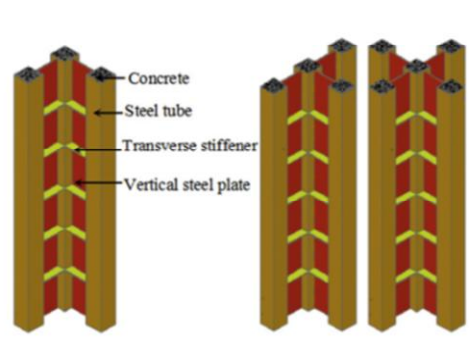

Fig. 6. Single vertical steel plate connection

When comparing the SCFST columns connected by lacing bars and those with single vertical steel plates, steel plates have a higher confinement of the lateral deflections and thus vertical steel plate connection have a much better property than lacing bar connection. However, SCFST connected by single vertical steel plates cannot meet the requirements of high-rise steel housing construction in terms of the bearing capacity and welding transverse stiffeners, complicating their application in rapid industrial construction processes. Double vertical steel plates connection pattern not only helps improve the confinement of core concrete but also helps increase the

bearing capacity and flexural rigidity.

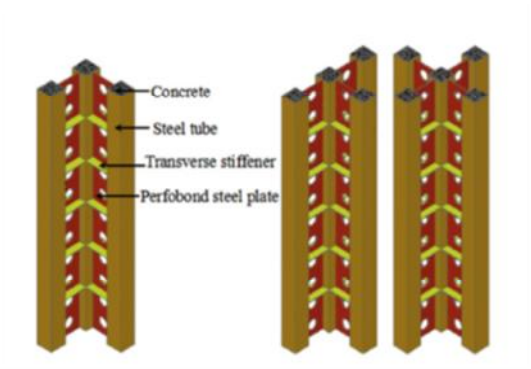

Fig. 7. Single vertical steel plate connection (with holes)

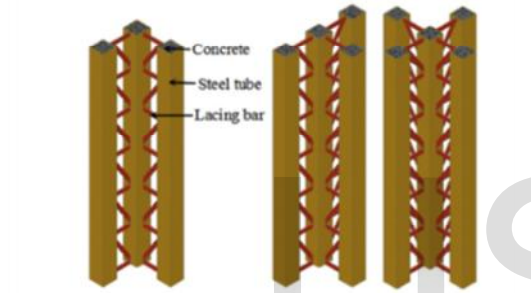

Fig. 8. Lacing bar connection

4 XCFST MODEL

XCFST column consist of five mono columns connected using a connection. Here, the connection chosen is double vertical steel plate connection. The specimens were modelled and analyzed using the commercially available finite element software, ANSYS 16.2. Four main components must be modelled to simulate the behaviour of XCFST columns: steel tubes, connection plates, inner-filled concrete, and the interface between

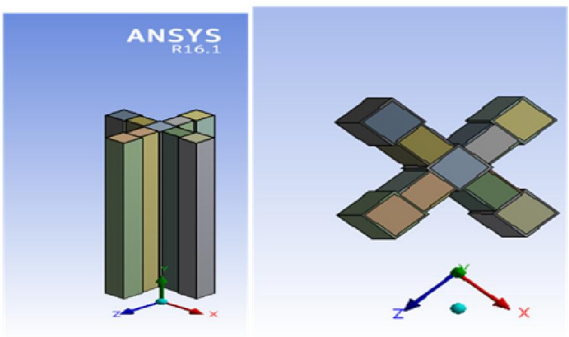

Fig.9. Isometric view and top view

TABLE 1
PROPERTIES OF STRUCTURAL CONCRETE

CONCRETE	
Compressive strength, f_{ck}	32.4 MPa
Elastic modulus, E_c	$3x10^4$ MPa
Poisson's ratio	0.15

the concrete and the steel tube. In addition, the selection for element type, mesh size, initial geometric deformation, boundary conditions and load application is also important in simulating the XCFST columns.

Mechanical properties are tabulated in Table 1 and Table 2. The contact between the steel plate and the concrete was simulated using the contact element and the friction coefficient was 0.25, as recommended by Wang Zhang et al. [6]. All the elements were modelled as solid elements. Default mesh size was given for the models. Boundary condition is given as, the top of the column was constrained in the X and Z displacement directions. Rotation about the X-axis, Y-axis and Z-axis was constrained. The bottom of the column was constrained in the three (X, Y and Z) displacement directions; in addition, the

TABLE 2
PROPERTIES OF STEEL TUBE AND STEEL PLATE

	STEELTUBE	STEELPLATE
Yield strength, f_y	380 MPa	368 MPa
Ultimate strength, f_u	475 MPa	439 MPa
Elastic modulus, E_s	$2.01x10^5$ MPa	$1.76x10^5$ MPa
Poisson's ratio	0.30	0.30

rotation about the Y-axis was constrained.

5 PARAMETER ANALYSIS

There is no doubt that the full scale physical testing is more reliable. As the engineering systems get complicated day by day, a better understanding of such systems is pivotal to their correct design and fabrication. However, in such cases the experimental approach suffers from various drawbacks such as limited capacity of instruments, significance increase in the cost of materials and data acquisition systems and so on. For example, due to the high load capacity of specimens, the capacity of loading machine can become a major issue in testing of SCFST columns. Therefore, most of the researchers have performed tests on limited scale for such columns, due to which there is lack of knowledge regarding behaviour of SCFST columns. With simulations, engineers are able to over-

come most of these problems, as these are time and cost-friendly, and need no special instrumentations. Nonetheless, research on this type of XCFST column is limited to date, and a large number of relevant parameters have yet to be investigated. We have no knowledge on designing the width, thickness and length of the column and other similar parameters. Thus, the aim of present parametric study is to simulate XCFST columns by studying the parameters, width and thick

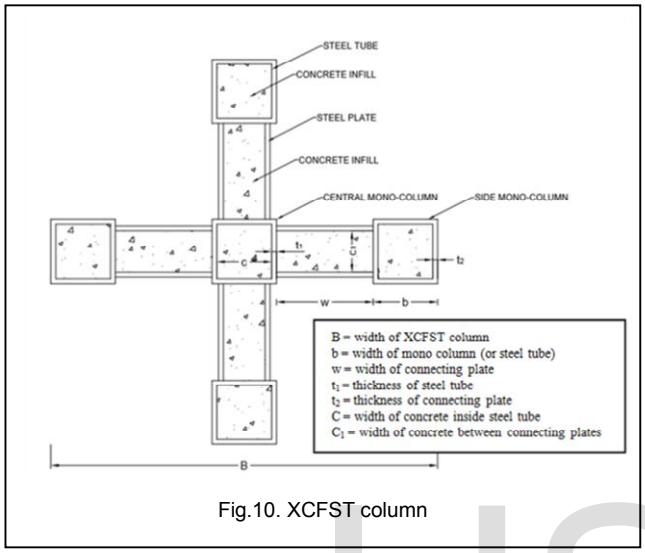

Fig.10. XCFST column

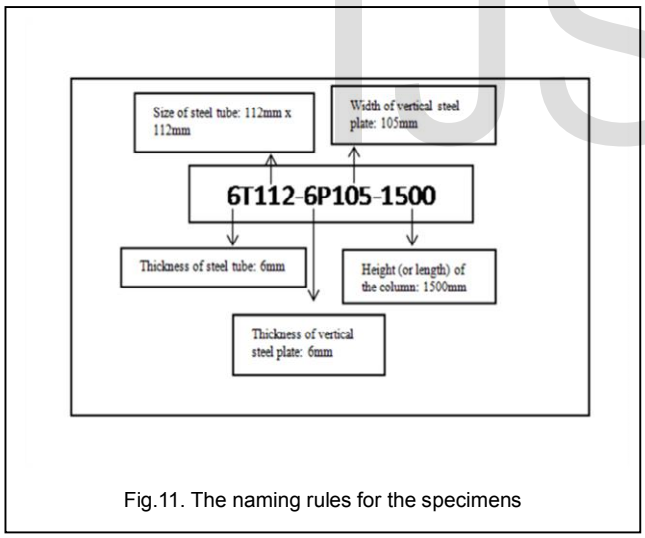

Fig.11. The naming rules for the specimens

ness of connecting plate and length of XCFST column connected using double vertical steel plate connection. A cross sectional view of an XCFST column and the related parameters are shown in Fig. 10

To conduct the study, specimens are grouped into different sets. Each specimen is named as it shows its dimensional properties. The naming rule chosen for the specimens is given in Fig. 11

6 EFFECT OF WIDTH OF CONNECTING PLATES

For the well functioning of the whole column, the connection between these mono columns should be sufficiently strong. Width of connecting plates plays a vital role in holding the mono columns altogether to act as a single column. There are no design codes available for fixing such parameters in XCFST columns. So, it is a necessity to find out the maximum allowable limit for the width of connecting plates or in other words, maximum allowable distance between two mono columns.

In the specimens chosen here, concrete area inside the tube and that between the connecting plates is kept constant. This is to avoid the effects due the variation in core concrete area. Widths for connecting plates are selected manually in such a way that, it will occupy the constant concrete area and also meets the space for welding at the end of the tube. Models are grouped into 4 sets; G1, G2, G3 and G4. Each group is a set of specimens having constant concrete area and constant column length.

6.1 Details of Models

In G1, steel tube (t_1) and connecting plate thicknesses (t_2) are 6 mm, 8 mm and 10 mm. There tried different combinations of thicknesses and 7 widths. Length of all the specimens is 1500 mm. To reduce the complexity, concrete area inside the tube and plates are made constant. G1 models have concrete area inside tube (Act): 10000 mm² i.e, C x C = 100 mm x 100 mm and concrete area in-between plates (A_{cp}): 8400 mm². Connecting plate widths chosen are 105 mm, 120 mm, 140 mm, 168 mm, 210 mm, 240 mm and 280 mm. These widths are selected in such a way that, the area of concrete in-between the connecting plates is 8400 mm².

TABLE 3
DETAILS OF GROUP G1A

SL NO	NAME	b mm	B mm	w mm	t_2 mm	C_1 mm
1	6T112-6P105-1500	112	546	105	6	80
2	6T112-8P105-1500	112	546	105	8	80
3	6T112-10P105-1500	112	546	105	10	80
4	6T112-6P120-1500	112	576	120	6	70
5	6T112-8P120-1500	112	576	120	8	70
6	6T112-10P120-1500	112	576	120	10	70
7	6T112-6P140-1500	112	616	140	6	60
8	6T112-8P140-1500	112	616	140	8	60
9	6T112-10P140-1500	112	616	140	10	60
10	6T112-6P168-1500	112	672	168	6	50
11	6T112-8168-1500	112	672	168	8	50
12	6T112-10P168-1500	112	672	168	10	50
13	6T112-6P210-1500	112	756	210	6	40
14	6T112-8P210-1500	112	756	210	8	40
15	6T112-10P210-1500	112	756	210	10	40
16	6T112-6P240-1500	112	816	240	6	35
17	6T112-8P240-1500	112	816	240	8	35
18	6T112-10P240-1500	112	816	240	10	35
19	6T112-6P280-1500	112	896	280	6	30
20	6T112-8P280-1500	112	896	280	8	30
21	6T112-10P280-1500	112	896	280	10	30

G1 is again categorised into 3 groups; G1A (Table 3), G1B (Table 4) and G1C (Table 5).

G1A is a set of specimens having tube thickness 6 mm and plate thickness 6 mm, 8 mm and 10 mm, for each connecting plate width. Similarly, for G1B tube thickness is 8 mm and for

TABLE 4
DETAILS OF GROUP G1B

SL NO	NAME	b mm	B mm	w mm	t_2 mm	C_1 mm
1	8T116-6P105-1500	116	558	105	6	80
2	8T116-8P105-1500	116	558	105	8	80
3	8T116-10P105-1500	116	558	105	10	80
4	8T116-6P120-1500	116	588	120	6	70
5	8T116-8P120-1500	116	588	120	8	70
6	8T116-10P120-1500	116	588	120	10	70
7	8T116-6P140-1500	116	628	140	6	60
8	8T116-8P140-1500	116	628	140	8	60
9	8T116-10P140-1500	116	628	140	10	60
10	8T116-6P168-1500	116	684	168	6	50
11	8T116-8P168-1500	116	684	168	8	50
12	8T116-10P168-1500	116	684	168	10	50
13	8T116-6P210-1500	116	768	210	6	40
14	8T116-8P210-1500	116	768	210	8	40
15	8T116-10P210-1500	116	768	210	10	40
16	8T116-6P240-1500	116	828	240	6	35
17	8T116-8P240-1500	116	828	240	8	35
18	8T116-10P240-1500	116	828	240	10	35
19	8T116-6P280-1500	116	908	280	6	30
20	8T116-8P280-1500	116	908	280	8	30
21	8T116-10P280-1500	116	908	280	10	30

G1C, 10 mm. Details of G1A, G1B and G1C are given in Table 3, Table 4 and Table 5, respectively.

TABLE 5
DETAILS OF GROUP G1C

SL NO	NAME	b mm	B mm	w mm	t_2 mm	C_1 mm
1	10T120-6P105-1500	120	570	105	6	80
2	10T120-8P105-1500	120	570	105	8	80
3	10T120-10P105-1500	120	570	105	10	80
4	10T120-6P120-1500	120	600	120	6	70
5	10T120-8P120-1500	120	600	120	8	70
6	10T120-10P120-1500	120	600	120	10	70
7	10T120-6P140-1500	120	640	140	6	60
8	10T120-8P140-1500	120	640	140	8	60
9	10T120-10P140-1500	120	640	140	10	60
10	10T120-6P168-1500	120	696	168	6	50
11	10T120-8P168-1500	120	696	168	8	50
12	10T120-10P168-1500	120	696	168	10	50
13	10T120-6P210-1500	120	780	210	6	40
14	10T120-8P210-1500	120	780	210	8	40
15	10T120-10P210-1500	120	780	210	10	40
16	10T120-6P240-1500	120	840	240	6	35
17	10T120-8P240-1500	120	840	240	8	35
18	10T120-10P240-1500	120	840	240	10	35
19	10T120-6P280-1500	120	920	280	6	30
20	10T120-8P280-1500	120	920	280	8	30
21	10T120-10P280-1500	120	920	280	10	30

TABLE 6
DETAILS OF GROUP G2

SL NO	NAME	b mm	B mm	w mm	t_2 mm	C_1 mm
1	6T162-6P105-2000	162	696	105	6	80
2	6T162-6P120-2000	162	726	120	6	70
3	6T162-6P140-2000	162	766	140	6	60
4	6T162-6P168-2000	162	822	168	6	50
5	6T162-6P210-2000	162	906	210	6	40
6	6T162-6P240-2000	162	966	240	6	35
7	6T162-6P280-2000	162	1046	280	6	30
8	6T162-6P336-2000	162	1158	335	6	25
9	6T162-6P420-2000	162	1326	420	6	20

G2 is a set of models having both the tube thickness, (t_1) and plate thickness, (t_2): 6 mm; Concrete area inside the tube, A_{ct}: 22500 mm² i.e, C x C = 150 mm x 150 mm; concrete area between plates, A_{cp}: 8400 mm² and length, L: 2000 mm. Connecting plate widths chosen are 105mm, 120mm, 140mm, 168mm, 210mm, 240mm, 280mm, 336 mm and 420 mm. Details of G2 is given in Table 6.

TABLE 7
DETAILS OF GROUP G3

SL NO	NAME	b mm	B mm	w mm	t_2 mm	C_1 mm
1	6T87-6P70-1000	87	401	70	6	50
2	6T87-6P100-1000	87	461	100	6	35
3	6T87-6P125-1000	87	511	125	6	28
4	6T87-6P140-1000	87	541	140	6	25
5	6T87-6P175-1000	87	611	175	6	20
6	6T87-6P250-1000	87	761	250	6	14

G3 is a group of models having both tube thickness, t_1 and plate thickness, t_2: 6 mm; A_{ct}: 5625 mm2 i.e, C x C = 75 mm x 75 mm; A_{cp}: 3500 mm2 and L = 1000 mm. Connecting plate widths are 70 mm, 100 mm, 125 mm, 140 mm, 175 mm and 250 mm. These widths are selected in such a way that concrete areas between the plates are kept constant as 3500 mm². Details of G3 are given in Table 7.

TABLE 8
DETAILS OF GROUP G4

SL NO	NAME	b mm	B mm	w mm	t_2 mm	C_1 mm
1	6T62-6P100-800	62	386	100	6	31
2	6T62-6P124-800	62	434	124	6	25
3	6T62-6P155-800	62	496	155	6	20
4	6T62-6P310-800	62	806	310	6	10

In G4, both t_1 and t_2: 6 mm; A_{ct}: 2500 mm² i.e, C x C = 50 mm x 50 mm; A_{cp}: 3100 mm² and L=800mm. Connecting plates widths are 100mm, 124mm, 155mm and 310 mm. Details are given in Table 8.

6.2 Maximum Allowable Ratio between w and b

Connecting plate width or distance between two mono columns is one of the most important factors that contribute the ultimate strength of XCFST column. Since, there are no design considerations available for the design of XCFST column, it is mandatory to find a maximum limit upto which the width of connecting plates can be given. Here, the maximum allowable ratio between connecting plate width (w) and mono column width (b) is found out using the behaviour of load-deformation curves of ANSYS models. A total of 82 models (G1, G2, G3 and G4) were modelled and analysed using ANSYS Workbench structural platform, to study the effect of width of connecting plates on load carrying capacity of XCFST column and thus defined the maximum allowable w/b ratio. Non-linear analysis was carried out for the models and load-deformation curves were obtained. From each group, load-deformation curves are plotted for similar tube thickness and similar plate thickness. This is to study the behaviour of columns with respect to the variation in width of connecting plates. From these load-deformation curves, ultimate load for each specimen is found out. w/b ratios are also calculated for every specimen. Using the ultimate load and w/b ratios, curves are drawn to conclude on the maximum allowable w/b ratio.

Results and Discussions

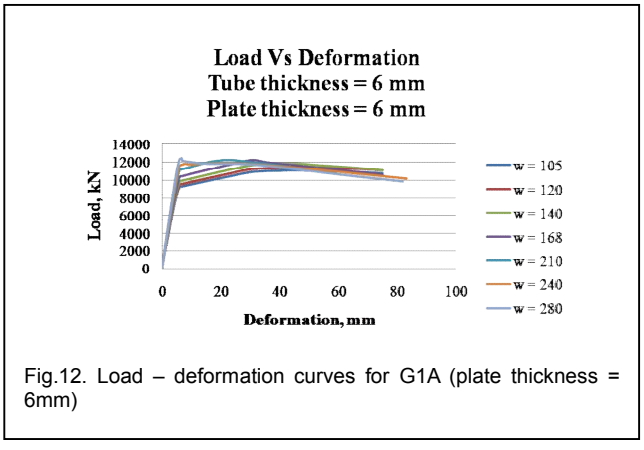

Fig.12. Load – deformation curves for G1A (plate thickness = 6mm)

In Fig.12, load-deformation curves are plotted for tube thickness 6 mm and plate thickness 6 mm with respect to seven widths chosen. In this plot, initially the load curve was increasing with the increase in connection plate width. After a width of 240 mm, there occurs a sudden fall in the load curve. Similar pattern of curves are obtained for other plate thicknesses in group G1A (Fig. 13 and Fig. 14). After 240 mm width, connecting plates fails to hold the mono columns as a single column. This shows that, 240 mm is the maximum allowable width that can be given for connecting plates for a tube width of 112 mm.

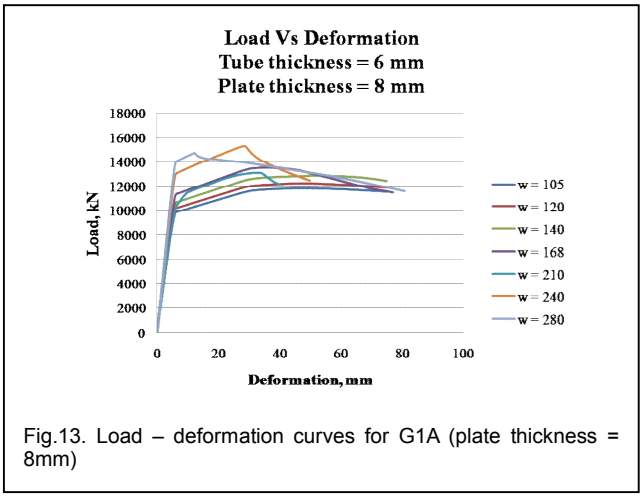

Fig.13. Load – deformation curves for G1A (plate thickness = 8mm)

Fig. 15 shows the load-deformation curves for tube thickness 8 mm and plate thickness 6mm for each plate width. The behaviour of columns was the same as for the group G1A. Initial increase in load was found out with the increase in plate width. After 240 mm plate width, sudden failure occurs to the columns, shows that the connecting plate loses its binding capacity. Similar pattern was occurred for the curves of plate thickness 8mm (Fig. 16) and 10mm (Fig. 17). Here also, the maximum allowable plate width found out is 240 mm for mono column width of 116 mm.

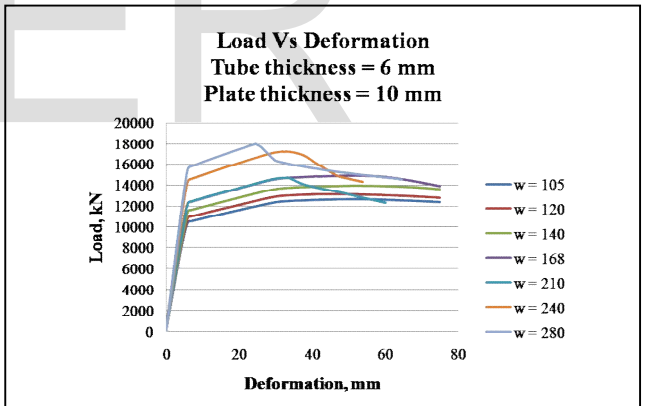

Fig.14. Load – deformation curves for G1A (plate thickness = 10mm)

Similarly, for set G1C initial increase in load was found upto a plate width of 240mm and after that a sudden fall occurred. Fig.18, Fig.19 and Fig.20 shows the pattern of load-deformation curves for the set G1C. Maximum allowable width is 240mm for mono column width 120 mm.

From the load-deformation curves of G1A, G1B and G1C, the maximum allowable plate width found was 240 mm. This is approximately double the mono column widths of these groups.

Fig.21 explains the behaviour of columns in G2, with increase in plate width. When comparing with set G1, G2 has a greater concrete area inside the steel tube. Here, the fall in load curve occurred after the width of 280 mm. Width of mono col-

umn is 162 mm. 280 mm is approximately double the width of mono column.

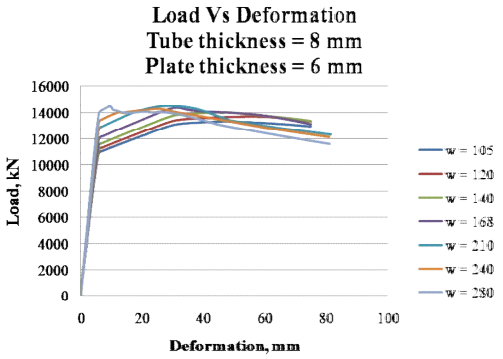

Fig.15. Load – deformation curves for G1B (plate thickness = 6mm)

In G3, a fall occurred after the width 175mm (Fig.22). G3 has a mono column width of 87 mm. So, after the plate width 175 mm, connecting plates lost its binding capacity to hold the mono columns altogether. Thus, the maximum allowable plate width for a tube width 87 mm is 175 mm, which is double the tube width.

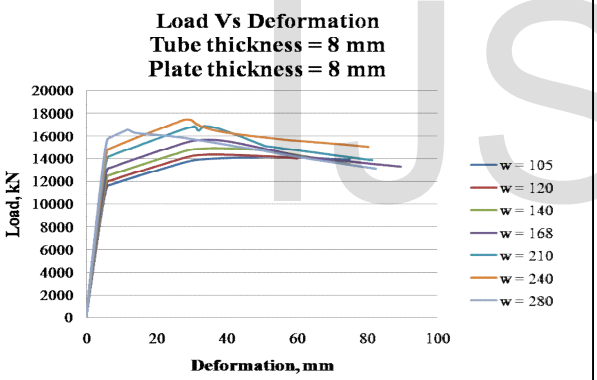

Fig.16. Load – deformation curves for G1B (plate thickness = 8mm)

For G4, mono column width is 62 mm. Fall occurred after the plate width of 124 mm. Here also, plate width is double the width of mono column. Fig.23 shows the behaviour of G4.

From the load-deformation curves of G1, G2, G3 and G4, the ultimate load for each specimen is found out. w/b ratios for each specimen were calculated.

Using these w/b ratios and ultimate load values, curves are plotted. Fig.24, Fig.25, Fig.26, Fig.27, Fig.28 and Fig.29 are the load-w/b curves of G1A, G1B, G1C, G2, G3 and G4 respectively.

From load-w/b curves (Fig.24, Fig.25, Fig.26, Fig.27, Fig.28 and Fig.29) it is evident that, a fall in ultimate load carrying capacity of XCFST columns occurs after the w/b ratio 2. It shows that the maximum distance between the columns that can be allowed is double the width of mono-column; i.e, w/b ≤ 2.

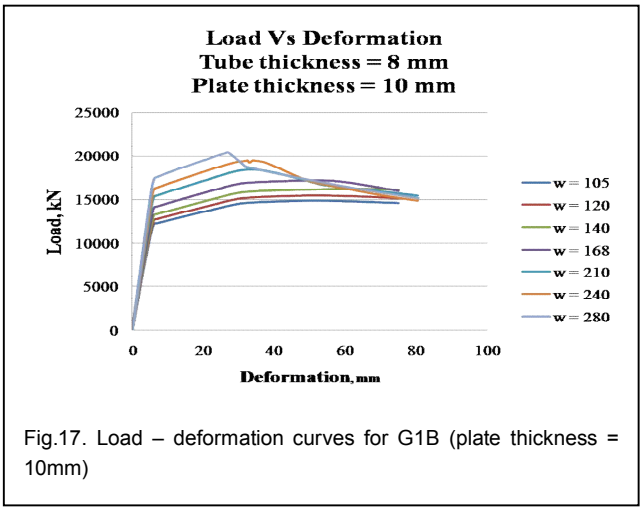

Fig.17. Load – deformation curves for G1B (plate thickness = 10mm)

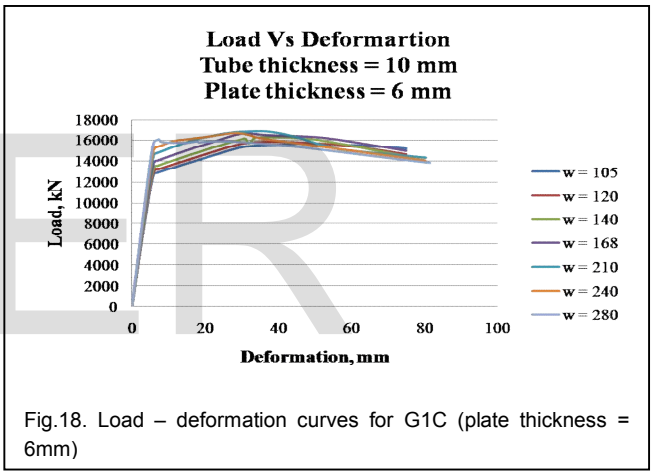

Fig.18. Load – deformation curves for G1C (plate thickness = 6mm)

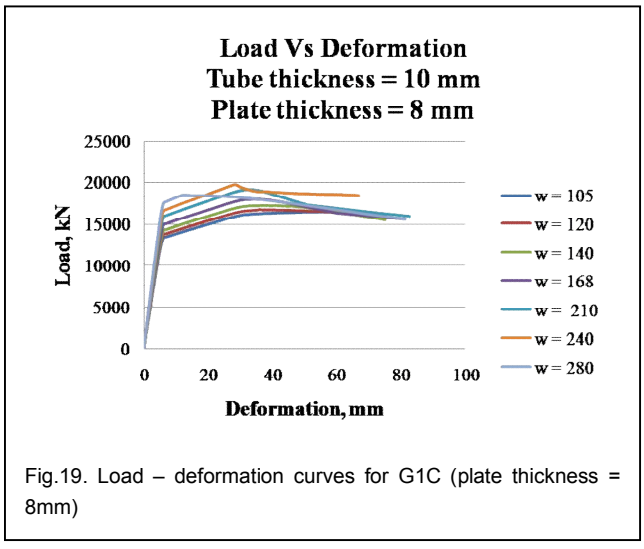

Fig.19. Load – deformation curves for G1C (plate thickness = 8mm)

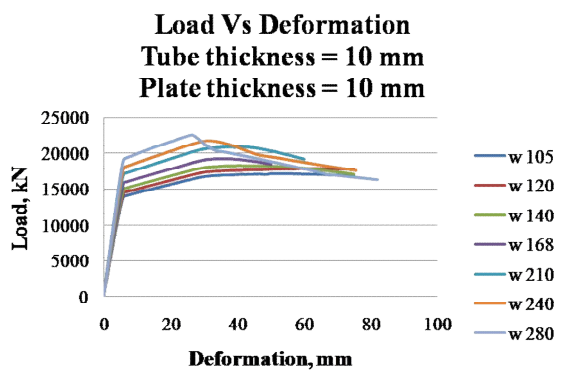

Fig.20. Load – deformation curves for G1C (plate thickness = 10mm)

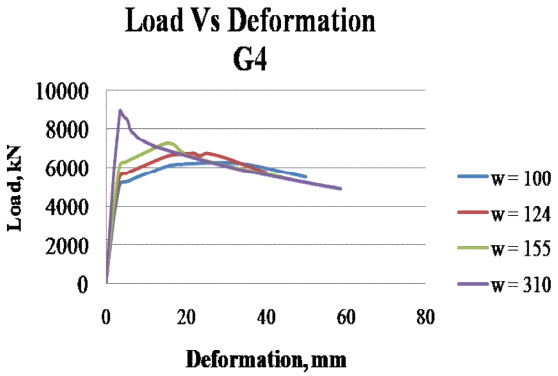

Fig.23. Load – deformation curves for G4

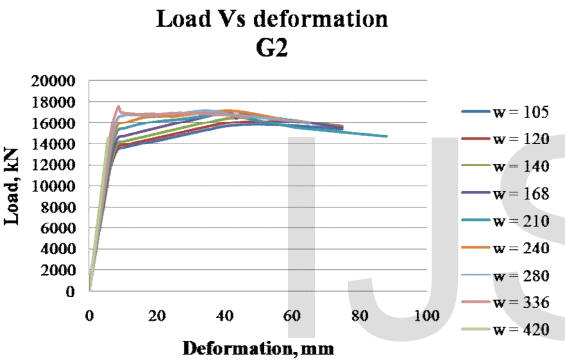

Fig.21. Load – deformation curves for G2

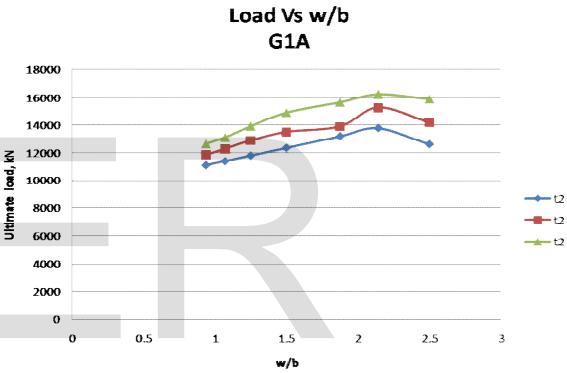

Fig.24. Load – w/b curves for G1A

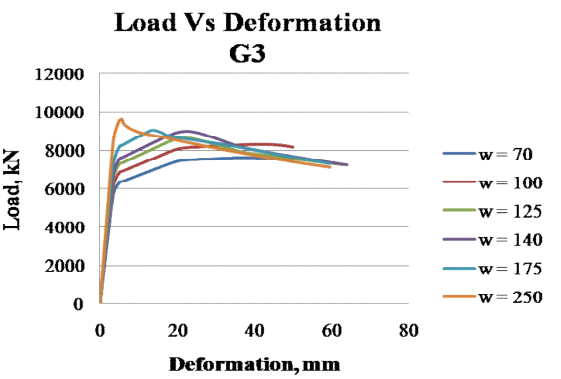

Fig.22. Load – deformation curves for G3

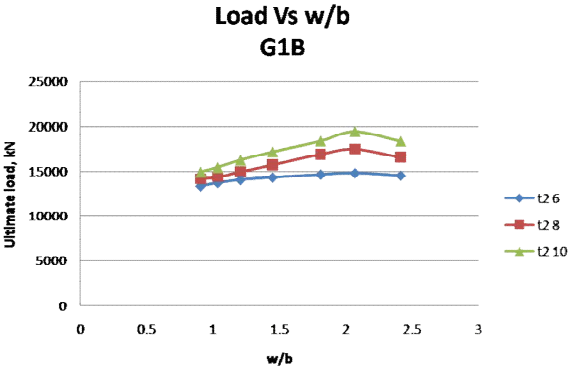

Fig.25. Load – w/b curves for G1B

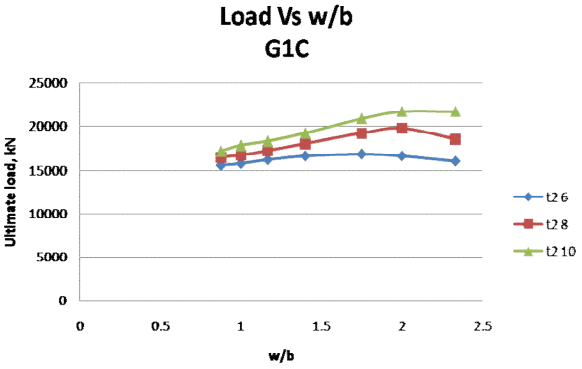

Fig.26. Load – w/b curves for G1C

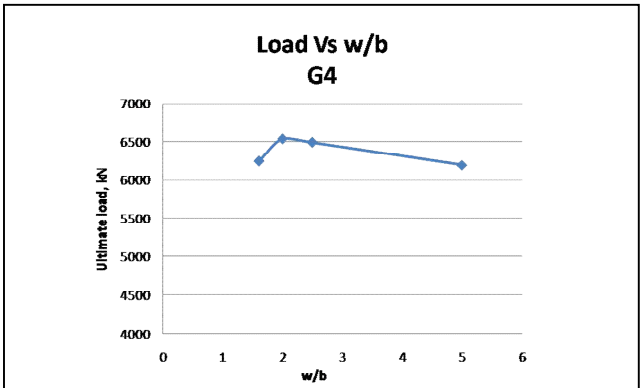

Fig.29. Load – w/b curves for G4

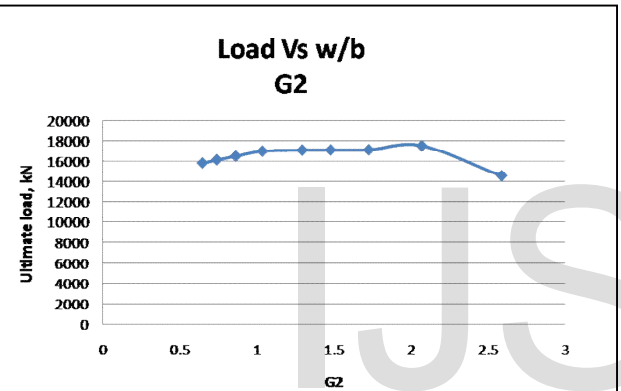

Fig.27. Load – w/b curves for G2

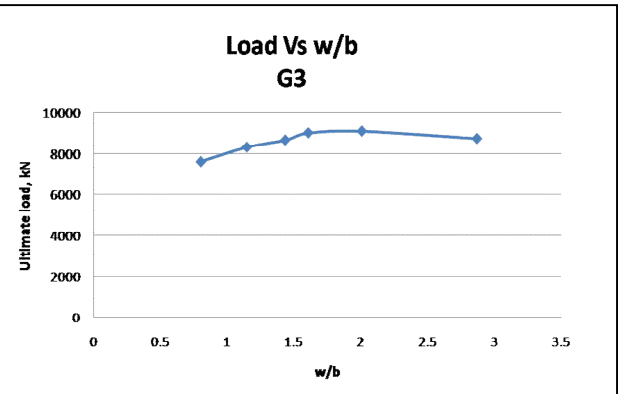

Fig.28. Load – w/b curves for G3

6.3 Maximum Allowable Ratio between L and B

Since, there are no design codes available for the design of XCFST columns, there is no knowledge on the maximum overall breadth that can be permitted for a given length of column. As the overall breadth of the column is the summation of width of monocolumn and that of connecting plate, previous inferences over the w/b ratio can be made use here. From each set of models (G1A, G1B, G1C, G2, G3 and G4) a maximum allowable plate width (w) was able to identify. Thus, the overall width (B) corresponding to this plate width can be taken as the allowable overall breadth. Taking the ratio L/B corresponding to this breadth can be chosen as the allowable maximum L/B ratio.

The same set of models (G1A, G1B, G1C, G2, G3 and G4) is used here, to reach the inference. Specimen details are given in Table 3, Table 4, Table 5, Table 6, Table 7 and Table 8.

Results and Discussions

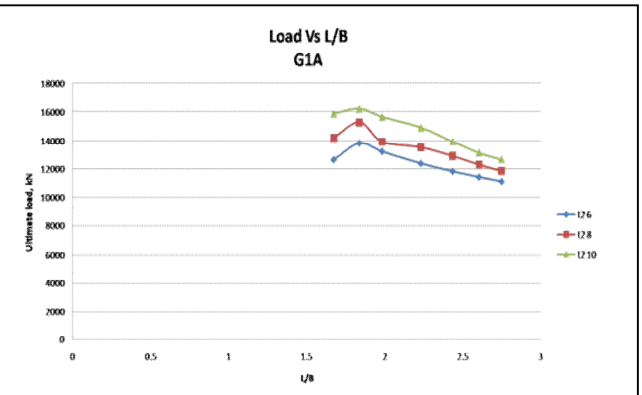

Fig.30. Load – L/B curves for G1A

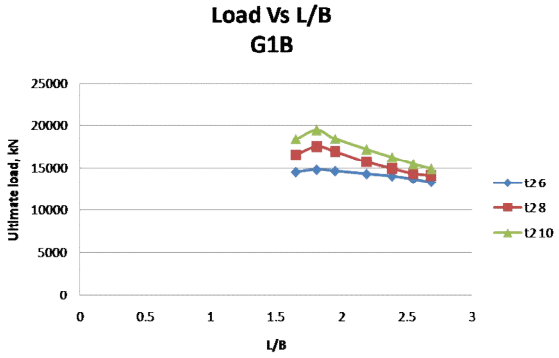

Fig.31. Load – L/B curves for G1B

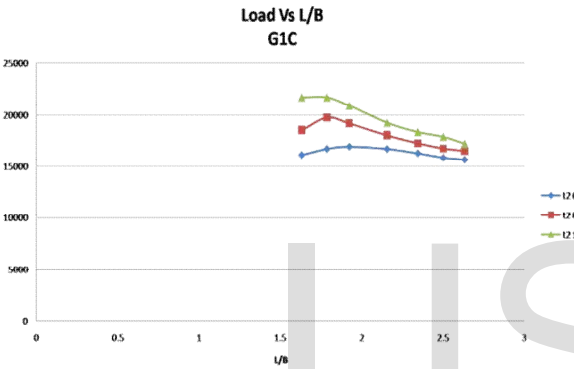

Fig.32. Load – L/B curves for G1C

For each specimen, ultimate load is obtained from the load-deformation curves obtained from FEM analysis. Using ultimate load values and L/B ratios, graphs are plotted and are shown in Fig. 30, Fig. 31, Fig. 32, Fig. 33, Fig. 34 and Fig. 35.

For set G1A, G1B and G1C, the maximum allowable plate width was 240 mm and corresponding overall breadths are 816 mm, 828 mm and 840 mm respectively. Thus the maximum allowable L/B ratios will be 1.84, 1.81 and 1.79. Fig.30, Fig. 31 and Fig. 32 also gives this conclusion. For L/B ratios greater than 1.8, column shows good performance. From this, it is clear that for the set G1, the maximum allowable L/B ratio is 1.8 i.e, for a given length, the maximum allowable overall width of a XCFST column is 1/1.8 times the length.

In the case of G2, G3 and G4, the maximum allowable plate widths were 280 mm, 175 mm and 124 mm and the corresponding overall column breadths are 1046 mm, 611 mm and 434 mm respectively. L/B ratios corresponding to these

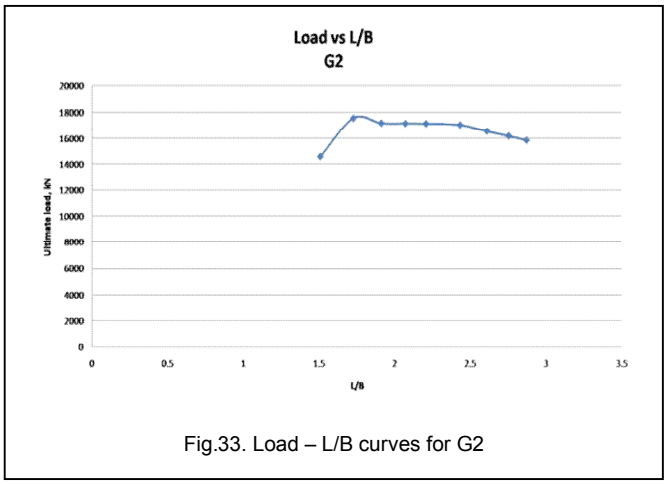

Fig.33. Load – L/B curves for G2

breadths are 1.91, 1.64 and 1.84. Here also, for L/B ratios greater than 1.8 column performs well and for less than 1.8 column fails. Fig. 33, Fig. 34 and Fig. 35 shows this pattern. Thus, for sets G2, G3 and G4 the maximum allowable L/B ratio is approximately 1.8.

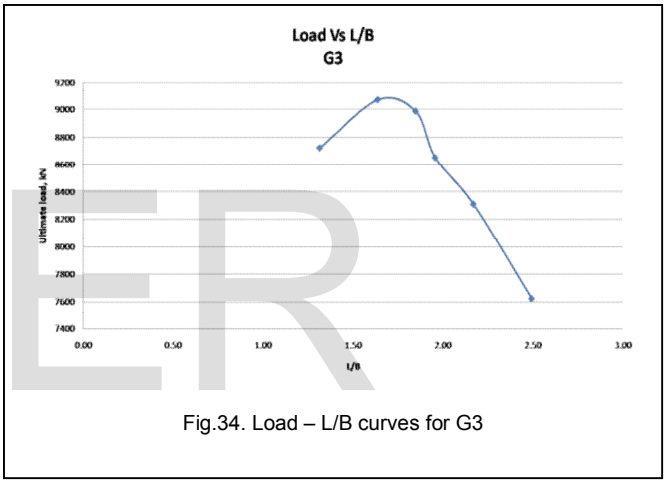

Fig.34. Load – L/B curves for G3

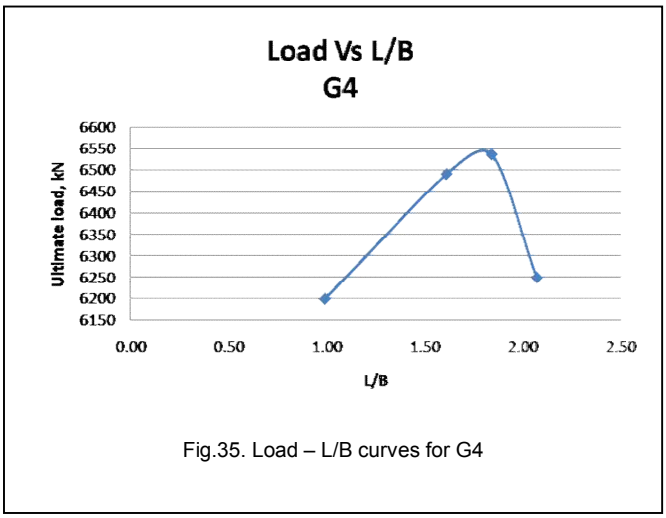

Fig.35. Load – L/B curves for G4

By analysing all the four sets of models, the arriving conclusion for the maximum allowable L/B ratio is that, for a given length of XCFST column, the maximum allowable

breadth of the column is 1/1.8 times the length. i.e, maximum allowable L/B ratio is 1.8.

7. CONCLUSION

Special shaped CFST columns are novel ideas and have wide acceptability due to their number of advantages. Only limited studies were carried out on these SCFST columns. Due to the lack of knowledge on the design criterias of SCFST columns, it is mandatory to conduct studies on this area. This paper aimed to conduct a study on cross shaped CFST column under axial loading using FEM analysis. Connection pattern between the mono columns opted was double vertical steel plates.

The following conclusions can be drawn based on the research work:

1) The influence of connecting plate size on bearing capacity was analyzed using FEM model.
2) Variation in the width of connecting plates reflects in the variations in the ultimate bearing capacity of XCFST column.
3) The maximum allowable ratio of connection plate width to tube width is 2.
4) For a given length of XCFST column, the maximum allowable overall breadth of the column is 1/1.8 times the length. i.e, L/B = 1.8.

REFERENCES

[1] Yongqian Zheng and Shaoxi Zeng, "Design of L-shaped and T-shaped concretefilled steel tubular stub columns under axial compression", *Elsevier, Engineering Structures*, 207,110262, 2020.

[2] Nithisha A and Abhishek CV, "Analytical performance of hybrid columns with CFST using Ansys workbench", *International Research Journal of Advanced Engineering and Science*, 493-497, 2019.

[3] Beena Kumari, "Concrete filled steel tubular (CFST) columns in composite structures", *IOSR Journal of Electrical and Electronics Engineering*, 13, 11-18, 2018.

[4] Fa-Cheng Wang and Lin-Hai Han, "Analytical behavior of special-shaped CFST stub columns under axial compression", *Elsevier,Thin-Walled Structures*, 129, 404–417, 2018.

[5] Y. Ouyang and A.K.H. Kwan, "Finite element analysis of square concrete-filled steel tube (CFST) columns under axial compressive load", *Elsevier, Engineering Structures*, 156, 443-459, 2018.

[6] Wang Zhang, Zhihua Chen and Qingqing Xiong, "Performance of L-shaped columns comprising concrete-filled steel tubes under axial compression", *Elsevier, Journal of Constructional Steel Research*, 145, 573-590, 2018.

[7] Zhi-Liang Zuoa, Jian Caia, Qing-Jun Chena, Xin-Pei Liu, Chun Yang and Ting-Wei Mo, "Performance of T-shaped CFST stub columns with binding bars under axial compression", *Elsevier, Thin Walled Structures*, 129, 183-196, 2018.

[8] Chen Qiguang, Cai Jian, Zuo Zhi Liang, Huang Jinxuan and Wei Jieying, "Study on cross-shaped concrete filled steel tubular stub columns subjected to axial compression: experiments and design method", *The Open Civil Engineering Journal*, 11, 1-13, 2017.

[9] Qingqing Xiong, Zhihua Chen, Wang Zhang, Yansheng Du, Ting Zhou and Jingfu Kang, "Compressive behaviour and design of L-shaped columns fabricated using concrete-filled steel tubes", *Elsevier, Engineering Structures*, 152, 758-770, 2017.

[10] Minyang Xu, Ting Zhou, Zhihua Chena, Yanbo Li and Luke Bisby, "Experimental study of slender LCFST columns connected by steel linking plates", *Elsevier, Journal of Constructional Steel Research*, 127, 231-241, 2016.

[11] J.Y. Richard Liew, Mingxiang Xiong and Dexin Xiong, "Design of concrete filled tubular beam-columns with high strength steel and concrete", *Elsevier, Structures*, 2016.

[12] Ting Zhou, Minyang Xu, Xiaodun Wang, Zhihua Chen and Ying Qin, "Experimental study and parameter analysis of L-shaped composite column under axial loading", *Springer, International Journal of Steel Structures*, 15(4): 797-807,2015.

[13] Yuanlong Yang, Yuyin Wang, Feng Fu and Jingchen Liu, "Static behavior of Tshaped concrete-filled steel tubular columns subjected to concentric and eccentric compressive loads" *Elsevier, Thin Walled Structures*, 95, 374-388, 2015.

[14] Bhushan H. Patil and P. M. Mohite, "Parametric study of square concrete filled steel tube columns subjected to concentric loading", *Journal of Engineering Research and Applications*, 4, 109-112, 2014.

[15] Lin-Hai Han, Wei Li and Reidar Bjorhovde, "Developments and advanced applications of concrete-filled steel tubular (CFST) Structures: Members", *Elsevier, Journal of Constructional Steel Research*, 100, 211–228, 2014.

[16] Y .Q. Tu, Y. F. Shenand P. Li, "Behaviour of multi-cell composite T-shaped concrete filled steel tubular columns under axial compression", *Elsevier, Thin Walled Structures*, 85, 57-70, 2014.

[17] P.K. Gupta, Ziyad A Khaudhair and A.K. Ahuja, "3D numerical simulation of concrete filled steel tubular columns using Ansys", *https://www.researchgate.net/publication/317380097*.

[18] Ziyad A. Khaudhair, P.K. Gupta and A.K. Ahuja, "Parametric investigations on behaviour of square CFST columns," *International Conference of Innovations in Civil Engineering*, 107-110, 2013.

[19] RONG Bi, CHENZ hi-hua, APOSTOLOS Fafitis and YANG Nan," Axial compression behavior and analytical method of L-shaped column composed of concrete filled square steel tubes", *Journal of Tianjin University*, 18, 180-187, 2012.

[20] Brian Uy, Zhong Tao and Lin-Hai Han, "Behaviour of short and slender concrete filled stainless steel tubular columns", *Elsevier, Journal of Constructional Steel Research*, 67, 360-378, 2011.

[21] Chen Zhi-hua, Rong Bin and Apostolos Fafitis, "Axial compression stability of a crisscross section column composed of concrete-filled square steel tubes", *Journal of Mechanics of Materials and Structures*, 4, 1787-1798, 2009.